Oscillating Temperature Pulses During CO Oxidation on a Pd/Al_2O_3 Ring

M. A. Liauw, M. Somani, J. Annamalai, and D. Luss
Dept. of Chemical Engineering, University of Houston, Houston, TX 77204

Back-and-forth-moving temperature fronts separating regions with high and low temperatures (amplitudes up to 100 K) formed on a Pd on alumina ring during the atmospheric oxidation of carbon monoxide. The back-and-forth front movement reflects the intrinsic nonuniformity of the catalytic system and the impact of global coupling. The ignition and extinction fronts usually moved at different velocities, in agreement with theoretical predictions. Complex spatiotemporal patterns were observed due to small-amplitude temperature fronts that moved on the high-temperature region at a much higher velocity than the high-amplitude fronts. The qualitative motion features were affected by changes in the excess oxygen concentration. The nonuniform states existed mainly for feed conditions for which the only uniform state was an extinguished one.

Introduction

Nonlinear interactions of diffusion and reaction may lead to spatiotemporal patterns in a wide variety of systems (Mikhailov, 1990; Cross and Hohenberg, 1993; Zaikin and Zhabotinskii, 1970; Castets et al., 1990; Ertl, 1991; Lee et al., 1993; Graham et al., 1994). Two-variable activator–inhibitor models with a fast-reacting, slow-diffusing activator and a slow-reacting, fast-diffusing inhibitor have been helpful in analyzing and predicting this behavior in many reacting and living systems. Pattern evolution on heterogeneous catalytic surfaces under atmospheric conditions differs in some important aspects from those described by the reaction-diffusion model or others that account only for local variables. The catalyst temperature usually plays the role of the activator, and its diffusivity is much higher than that of the surface species, which is the inhibitor. Thus, only uniform states are expected by the two-variable diffusion-reaction model (Pismen, 1979). However, temperature patterns have been observed on catalytic wafers, gauzes, and pellets by Brown et al. (1985), Pawlicki and Schmitz (1987), Lobban and Luss (1989), Kellow and Wolf (1990; 1991), Lane et al. (1993), and Qin and Wolf (1994).

The observed stationary and rotating temperature pulses are usually stabilized by global interaction, that is, the system dynamic is also influenced by some nonlocal variable. A very simple example is the stabilization of temperature patterns on electrically heated ribbons kept at a fixed resistance or average temperature (Volodin et al., 1982; Sheintuch, 1989; Lobban et al., 1989; Garske and Harold, 1992) in which each point is affected by the average temperature of the ribbon. In a constant-temperature mixed vessel, global interaction arises naturally due to interaction between the catalytic surface and the mixed-gas concentration (Middya et al., 1994), which introduces a new mode of communication among distance surface elements. In a constant temperature reactor, the global interaction stabilizes patterns that would not exist in its absence for reactions with a monotonic rate dependence on the reactant concentration. For example, when a high-temperature region attempts to expand, the increased local reaction rate decreases the mixed-gas concentration, which, in turn, decreases the reaction rate at all points on the catalyst and arrests the growth of the high-temperature region. Simulations by Middya et al. (1994) and Middya and Luss (1995) revealed a rich variety of patterns, which were stabilized by the global interaction, on ring, ribbon, and disk catalysts.

Slin'ko and Jaeger (1994), Ertl and Imbihl (1995), and Sheintuch and Shvartsman (1996) reviewed pattern formation in catalytic systems. Patterns on two- and three-dimensional catalytic pellets are intricate and difficult to analyze and characterize. This motivated studies on pattern formation on simpler geometries, such as thin catalytic ribbons and rings.

Correspondence concerning this article should be addressed to D. Luss.

Present address of M. A. Liauw: Lehrstuhl für Technische Chemie I, Friedrich-Alexander Universität Erlangen-Nürnberg, Egerlandstrasse 3, 91058 Erlangen, Germany.

Observed patterns on electrically heated Pt ribbons include standing waves (Lobban et al., 1989), source points (Cordonier and Schmidt, 1989), antiphase oscillations (Cordonier et al., 1989), and back-and-forth motion (Philippou et al., 1991; Philippou and Luss, 1993). Patterns on catalytic rings are not influenced by end effects in contrast to those on ribbons, and this simplifies their analysis and simulations. Observed patterns on catalytic rings include rotating pulses (Lane and Luss, 1993; Yamamoto et al., 1995a), antiphase or domain oscillations (Graham et al., 1993; Somani et al., 1997), and stationary hot-spot (Somani et al., 1996).

An important feature of heterogeneous catalytic surfaces operating at atmospheric or higher pressures is their nonuniformity. This nonuniformity may be due to variations in the local catalytic activity and/or local transport properties. The nonuniformity may introduce many novel dynamic features, for example, on a nonuniformly active ring, the velocity and shape of a rotating pulse depends on the azimuthal position (Lane and Luss, 1993; Yamamoto et al., 1995a; Somani et al., 1997), causing periodic changes in the conversion. Rather unusual temperature patterns were observed on nonuniform ribbons (Lobban et al., 1989), and they may disguise the observed multiplicity patterns (Garske and Harold, 1992). Numerous recent theoretical studies examined the impact of nonuniformity on spatiotemporal patterns (Bär et al., 1994; Kulka et al., 1995; Haas et al., 1995; Schütz et al., 1995; Hagberg et al., 1996; Liauw et al., 1996a; Bangia et al., 1996). One goal of our study was to examine the impact of nonuniformity on the temperature patterns.

The only pattern observed so far on a supported ring catalyst was a stationary high-temperature region formed during hydrogen oxidation, under conditions that two different uniform states may exist (Somani et al., 1996). Experiments on metallic rings and simulations suggest that other patterns exist (Graham et al., 1993; Yamamoto et al., 1995a,b; Middya et al., 1994). Our goal was to observe some of these more "dynamic" patterns on supported rings in order to enhance our understanding of their evolution and stabilization, and the conditions leading to a transition (bifurcation) from a uniform to a patterned state. The local catalyst dynamics affect pattern selection (Middya et al., 1994; Middya et al., 1993; Sheintuch, 1989). The nonisothermal CO oxidation on supported Pt catalysts displays rate oscillations (Beusch et al., 1972; Plichta and Schmitz, 1979), in addition to the well-known bistability. Several mechanisms were proposed to explain this dynamic behavior, such as slow periodic oxidation-reduction, structural surface transformation, or surface facetting (Ertl, 1990; Schüth et al., 1993; Slin'ko and Jaeger, 1994; Choi and Vannice, 1991). Self-similar mixed-mode oscillations observed on supported Pd catalyst by Jaeger et al. (1986) and Slin'ko et al. (1989) were explained by a model accounting for nonuniform catalyst activity and gas-phase coupling (Liauw et al., 1996b). CO oxidation on Pt exhibits bistability and oscillations in the presence of external mass-transfer resistance (Garske and Harold, 1992). The reaction generates nonuniform temperature patterns on a supported Pd disk (Kaul and Wolf, 1985). These motivated us to study the formation of temperature patterns during CO oxidation on a Pd on γ-alumina catalyst ring.

In most observed patterns a rather sharp temperature front separates regions of high (ignited) and low (extinguished) temperatures. Many front features, such as its length and velocity, may be readily predicted if the catalyst has a uniform activity and the system dynamics may be described by a single-variable model, that is, the surface concentration is in pseudoequilibrium with catalyst temperature. In such cases, a stationary front exists only if (Busch, 1921; Barelko et al., 1978; Pismen, 1979),

$$\int_{T_1}^{T_2}[\dot{Q}_G(T,C)-\dot{Q}_R(T)]\,dT=0, \tag{1}$$

where T_1 and T_2 are the low and high uniform steady-state temperatures, $\dot{Q}_R(T)$ and $\dot{Q}_G(T,C)$ are the heat-removal and heat-generation rates that depend on the catalyst temperature, T, and the gas-phase reactant concentration, C.

The single-variable model enables prediction of the characteristic thermal length, that is, the length over which the temperature changes. Observations of temperature fronts during hydrogen oxidation on a supported nickel catalyst (Somani et al., 1996) did not agree with such estimates and the front length was about three times larger than that predicted by this model. This discrepancy was probably caused by the high rate of heat transport in the boundary layer of hydrogen that is not accounted for in this model. One of the goals of this study was to check if the predictions of that model would hold when the gas thermal-conductivity is low. In addition, the interaction between the oscillatory nature of CO oxidation over a supported Pd catalyst and global interaction strongly suggests the formation of interesting spatiotemporal patterns. Our goal was to observe these in order to enhance our understanding of pattern formation and selection.

Experimental System and Procedure

Experiments were conducted on a thin catalytic ring of Pd on γ-alumina. It was prepared by pressing (2 tons/cm^2) a palladium-on-alumina powder (1% Pd; Aldrich) in a die. Details of catalyst preparation were reported by Somani (1996). The catalytic ring had 27-mm-ID, 34-mm-OD, and 0.9-mm thickness. It was placed horizontally on the tips of four sheathed, iron-constantan thermocouple junctions (Omega) in a cylindrical stainless-steel reactor of 68-mm-ID and 39-mm height (Figure 1). The reactor lid was an infrared-transparent sap-

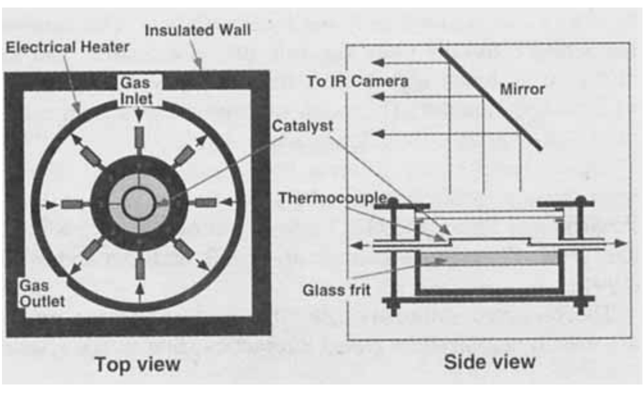

Figure 1. Reactor top (left) and side (right) view.

The feed enters the reactor through four inlet ports that are 90° apart. The outlet ports are shifted by 45°.

phire window (Union Carbide Crystals Division). The atmospheric reactor was placed inside an insulated oven, and a PID controller (Omega CN2041) maintained a constant reactor wall temperature.

An AGEMA (Thermovision 780) indium-antimonide (In-Sb) camera sensitive to 2–5.6 μm measured the temperature profile of the catalytic ring. A mirror was used to view the catalyst, as the camera had to be operated horizontally (Figure 1, right). The camera scanned a 5.6-cm × 4.6-cm field every 0.64 s with a spatial resolution of 0.3 mm^2. The 128×64 image matrix of local radiation levels (8-bit) was converted to local surface-temperature images, digitized, and recorded on a Mac II computer for later analysis.

The feed gases were prepurified-grade nitrogen (purity 99.998%) and extra-dry-grade oxygen (purity 99.6%) in stainless-steel cylinders and certified-grade mixture of 30 vol. % carbon monoxide and 70 vol. % nitrogen in an aluminum cylinder (Linde division of Union Carbide). An aluminum cylinder was chosen to avoid formation of carbonyls that could deactivate the catalyst. The carbon monoxide was passed through an in-line carbonyl trap of a molecular sieve adsorbent (Linde, 5A zeolite) kept at 240°C. The feed gases were mixed in a bed of glass beads, purified, and dried by in-line activated charcoal purifiers (Linde) before entering the reactor. Thermal mass-flow controllers (Tylan FC-280 and FC-260, accuracy $\pm 1\%$) were used to control the oxygen, nitrogen, and carbon monoxide flow rates. The total flow rate was 800 std. cm^3/min, which led to a residence time of about 6 s.

The gases were fed by four angularly symmetric inlet ports (2.4-mm-ID) located near the bottom of the reactor chamber, and the product gases exited through four similar outlet ports (4.7-mm-ID, shifted with respect to inlet ports by 45° and 13 mm upwards) near the top. A cylindrical glass frit (67-mm-dia., 6-mm-thick, 150-μm average pore size; Ace glass) placed between the catalyst and inlets distributed the feed gases. The effluent carbon monoxide concentration was continuously measured by an infrared analyzer (Anarad, AR-411). No reaction was observed in the empty (without catalyst) reactor at temperatures up to 200°C, which exceeded the experimental range of 30–180°C. Experiments repeated after several weeks were qualitatively, but not quantitatively reproducible. This behavior is typical for heterogeneous catalysts (see, e.g., Lynch and Wanke, 1984; Sheintuch and Schmidt, 1988; Graham et al., 1993).

No temperature variations in the radial direction were observed, indicating that the system may be treated as one-dimensional with periodic boundary conditions. Figures of surface temperature as a function of time and angular position were created by placing a series of one-dimensional temperature images next to each other.

Experimental Results

The experiments revealed that spatiotemporal temperature patterns form under certain conditions on a supported Pd catalyst ring during the oxidation of carbon monoxide. The experiments were conducted at two different feed oxygen concentrations of 4 and 70 vol. %, while the feed CO concentration was varied between 0 and 6 vol. %, with nitrogen being the rest. Carbon monoxide was the limiting component in all the experiments.

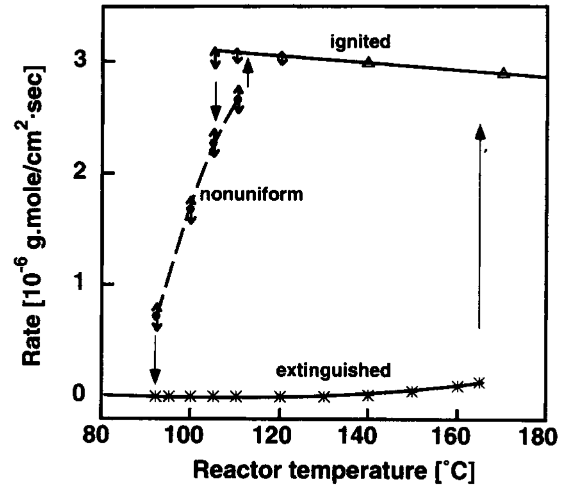

Figure 2. Bifurcation of the global reaction rate vs. reactor temperature for a feed containing 4 vol. % oxygen and 4 vol. % CO.

In addition to bistability of uniform states, a nonuniform state existed, and its reaction rate was bounded between those of the uniform states. Small oscillations on the ignited and nonuniform branch are shown by arrows.

The catalyst exhibited, for both feed oxygen concentrations, bistability of stationary states over a bounded region of composition and temperatures, that is, either a fully ignited or extinguished state existed for the same operating conditions. Figure 2 shows a typical hysteresis in the reaction rate for reactor temperature in the range of 105–167°C for a feed of 4 vol. % oxygen and 4 vol. % CO. The reaction rate on the low-temperature branch was negligible, and the catalyst temperature was very close to that of the reactor. The reaction rate on the fully ignited branch was high and the catalyst temperature was significantly higher than that of the reactor (60–70°C for a feed of 4 vol. % CO). The reaction rate on the ignited branch decreased slightly with increasing temperature, and small amplitude rate oscillations occurred close to the extinction point (Figure 2). The temperature of the fully ignited state was not uniform. The difference between the maximum and minimum surface temperature was of the order of 15°C when the average ring temperature exceeded by 65°C that of the ambient gas. A typical case is shown in Figure 3. This was probably caused by nonuniformities in the catalyst properties and transport coefficients. Rotating the ring by 180° had a minor influence on the temperature profile of a fully ignited state. This suggests that flow maldistribution had a predominant effect on the local net rate of heat generation. The temperature nonuniformity was more pronounced when the glass frit was absent.

In addition to the extinguished and fully ignited states, nonuniform states existed in which rather sharp temperature fronts separated regions with high and low catalyst temperatures (Figure 3). The temperature fronts moved back-and-forth, and both the length and amplitude of the high-temperature region changed, causing oscillations in the overall reaction rate. The average reaction rate increased with increasing reactor temperature and was always bounded between those of the uniformly ignited and extinguished states, that is, the uniform ignited state gave higher conversion than the nonuniform ones. The transitions from the ignited to the

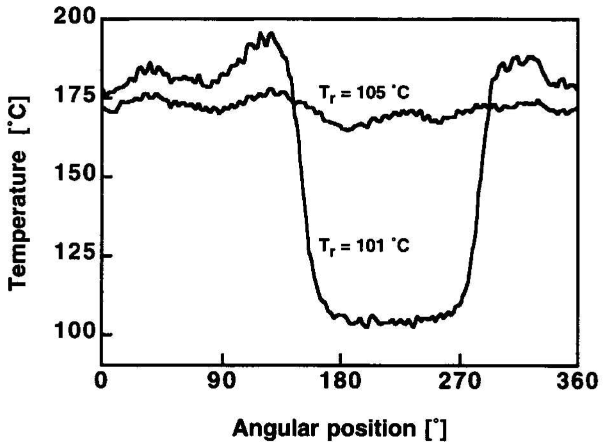

Figure 3. Temperature profiles of a fully ignited and a nonuniform state for a feed containing 4 vol. % oxygen and 4 vol. % CO.

Both profiles were recorded during the experiments described in Figure 4.

nonuniform state were different for oxygen feed concentrations of 4 and 70 vol. %.

For a feed of 4 vol. % oxygen, a nonuniform state in which sharp fronts separated regions with different temperatures was obtained from the fully ignited states by slowly decreasing the reactor temperature. The transition between the ignited and nonuniform states exhibited a hysteresis. Figure 2 shows a case in which the shift from the ignited to the nonuniform state occurred at 105°C. However, the nonuniform state ignited only when the reactor temperature exceeded 110°C. A typical scenario leading to such a temperature pulse formation is shown in Figure 4a for a reactor that was slowly cooled (0.17 K/min) from 110 to 100°C. At about 103°C, part of the catalyst extinguished. This, in turn, increased the reactor CO concentration (Figure 4b) and the temperature of the ignited section of the ring (Figure 3). Eventually, when the reactor temperature settled to 100°C, the temperature fronts caused about half of the ring to be at a high and half at a low temperature. The temperature of the cold part was close to that of the extinguished state, and that of the hot part close to that of an ignited state. Because the reaction rate of a nonuniform state is lower than that of an ignited state, the reactor concentration and temperature of the high-temperature region exceeded those of a fully ignited state (Figure 3) even though the reactor temperature was lower.

The spatiotemporal patterns reveal a back-and-forth movement of the temperature fronts. Figures 5a and 5b show such oscillating temperature fronts for a feed containing 4 vol. % CO and reactor temperatures of 105 and 95°C, respectively. The temperature fronts in this case tended to maintain a constant distance between them and to reverse direction at about the same instant. They moved at a velocity of about 0.04 cm/min. The short low-temperature region (pulse) which existed for reactor temperatures close to the extinction of the fully ignited branch (see Figure 5a), expanded with decreasing reactor temperature (see Figure 5b). The low (high)-temperature pulse moves back and forth within the region in which the temperature of the fully ignited state was low (high) (see Figure 5c).

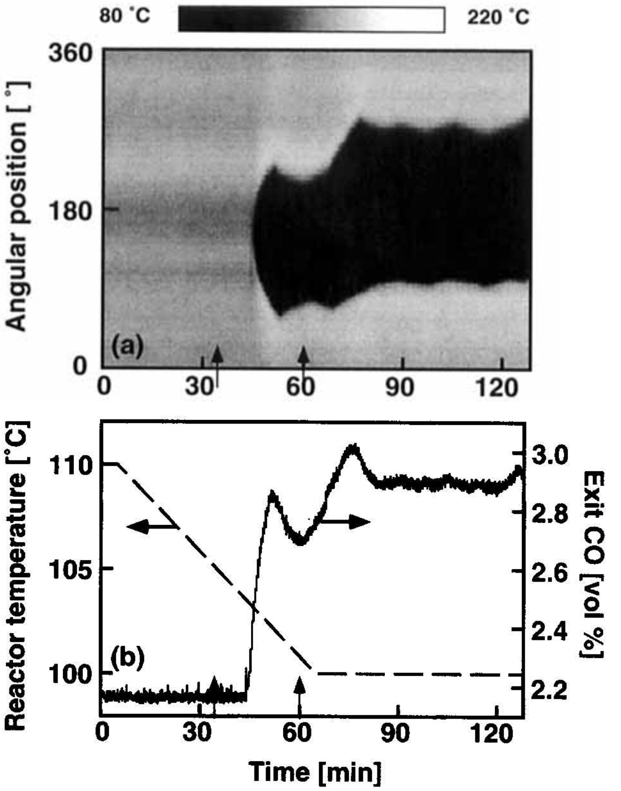

Figure 4. Autonomous formation of a nonuniform state for a feed containing 4 vol. % CO.

(a) Surface temperature as a function of time and angular position. (b) Corresponding reactor temperature and effluent oxygen concentration vs. time. The arrows on the abscissas indicate the times at which the profiles shown in Figure 3 were recorded.

Figure 6 shows that for a feed containing 5 vol. % CO, lowering the reactor temperature decreased the temperature of the cold region and increased the length of the cold region. This increased the reactor CO concentration and hence the temperature of the hot region. Since the pulse oscillated, we show instantaneous temperature profiles for reactor concentrations equal to the time average under the specific operating conditions.

A decrease of the CO concentration increased the length of the cold region and the reactor concentration, but had a negligible influence on the temperatures of the hot and cold regions (Figure 7). A slow increase in the reactor temperature or feed concentration, followed by a slow return to the initial conditions, sometimes shifted the location of the temperature fronts. A typical situation for which the fronts formed at one of the two locations is shown in Figure 8.

For a feed containing 70 vol. % oxygen, a slow decrease of the reactor temperature led to a gradual transition from the fully ignited to the nonuniform state without the hysteresis observed for 4 vol. %. Upon slow cooling, cold spots appeared intermittently on the fully ignited ring, followed by an eventual formation of an oscillating low-temperature pulse. Figure 9 describes a case in which the transition from a fully ignited state to a nonuniform state occurred over a temperature range of about 40°C. The catalyst was fully ignited at 110°C and local intermittent short dips in the catalyst tem-

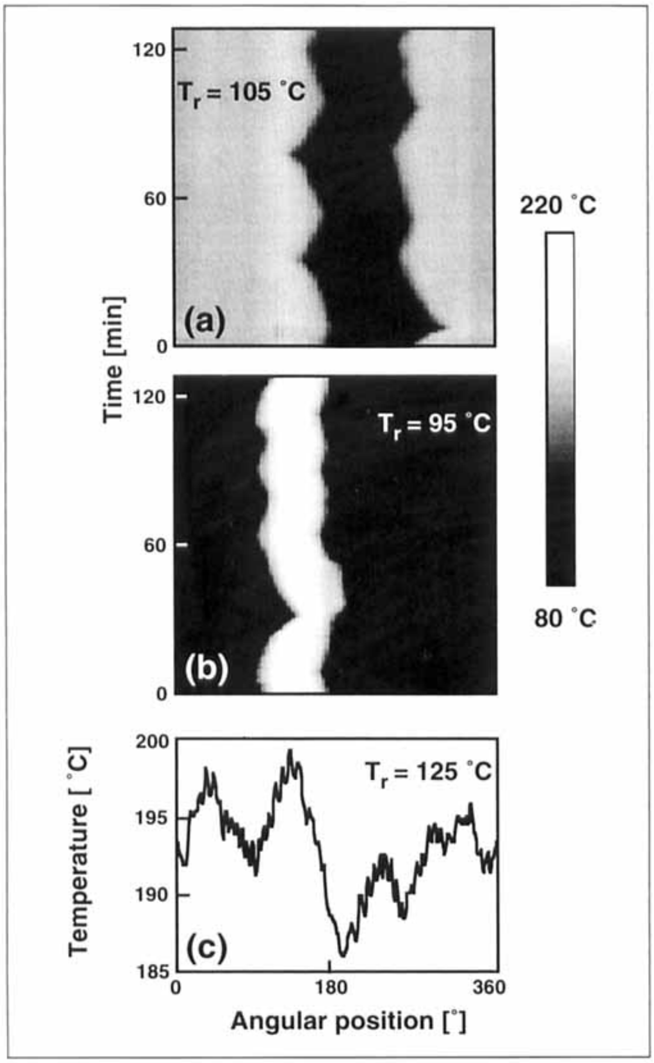

Figure 5. Surface temperature as a function of angular position and time for a feed containing 4 vol. % oxygen and 4 vol. % CO with a reactor temperature of (a) 105°C; (b) 95°C: (c) temperature profile of a fully ignited state.

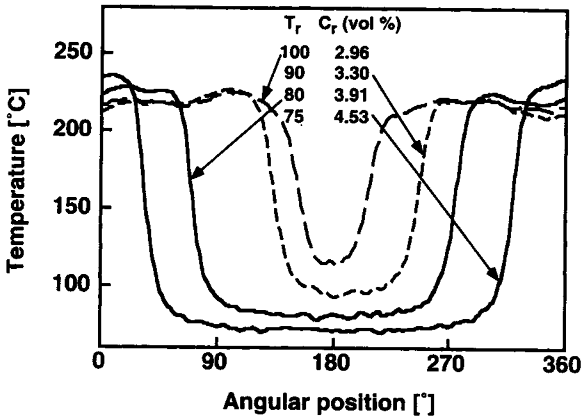

Figure 6. Temperature profile and corresponding average outlet concentration for different reactor temperatures for a feed containing 4 vol. % oxygen and 5 vol. % CO.

perature occurred at 95°C. We refer to these as *moving cold spots.* The amplitude and the rate of formation of the cold spots increased as the reactor temperature was decreased.

A permanent cold region formed when the reactor temperature was about 70°C (Figure 10a). Further cooling increased the size of the cold region between the fronts (Figures 10a, 10b), as in the experiments with 4 vol. % oxygen (Figure 6). However, at the higher oxygen concentration, the amplitudes of the fronts' spatial oscillations were larger and moving cold spots appeared and disappeared intermittently on the high-temperature region. These cold spots increased the amplitude of the rate oscillations over those obtained with 4 vol. % oxygen (compare Figures 11a and 11b).

The ignition fronts (which expand the ignited region with time) moved in general at a lower velocity than the extinction fronts. For example, Figure 10 shows that at the position 180°, the ignition- and extinction-front velocities were of the order of 0.07 and 0.2 cm/min, respectively. The two fronts did not reverse their direction of motion at the same instant. The fronts bounding the moving cold spots moved on the high-temperature region at a much higher velocity (order of 0.9 cm/min) than the high-amplitude fronts. In some instances the moving cold spots led to local extinction and splitting of a high-temperature pulse into two (Figure 10). In some cases, two pulses collided, forming a single pulse (Figure 10b), while in other cases, one of the high-temperature pulses extinguished (Figure 10c).

For a given feed-oxygen concentration, similar dynamic behavior and transitions from a fully ignited to extinguished branch were observed for different feed CO concentrations. Increasing the feed-oxygen concentration decreased both the ignition and extinction temperatures of both the bistable and nonuniform states (Figure 12). In the case of 70 vol. % oxygen, the transition from fully ignited to nonuniform state was assumed to be the temperature below which two temperature fronts existed at all times. For both oxygen concentrations, an increase of the feed CO concentration decreased the extinc-

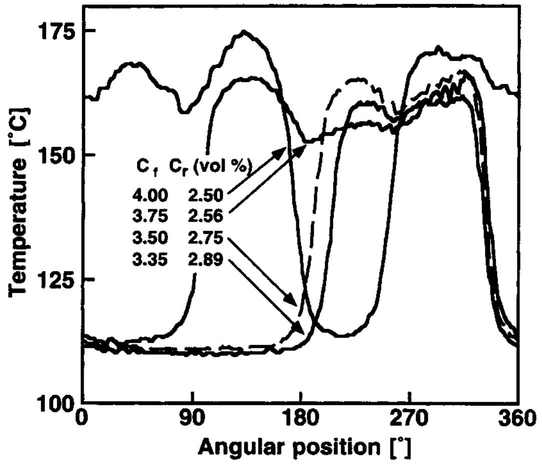

Figure 7. Temperature profile and corresponding average outlet concentration for oxygen feed concentration of 4 vol. %, reactor temperature of 110°C, and different CO feed concentrations.

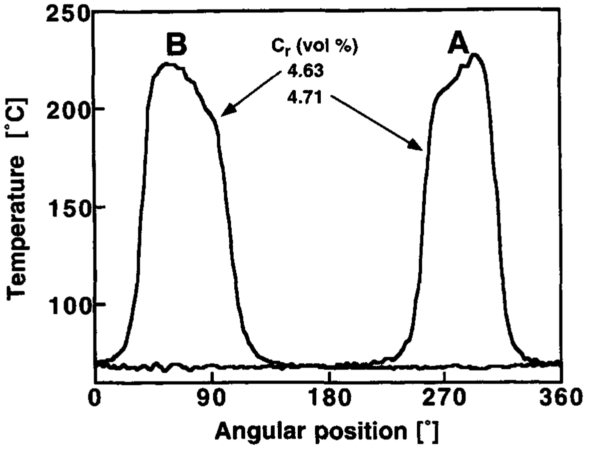

Figure 8. Temperature pulses at different locations for a reactor temperature of 70°C with 4 vol. % oxygen and 5 vol. % CO feed.

The pulse B was obtained by a slow increase of reactor temperature followed by a slow decrease to the initial level of pulse A.

tion temperature of the fully ignited state and increased the ignition temperature of the extinguished state. It decreased both the ignition and extinction temperatures of the nonuniform state, and increased the temperature range over which a nonuniform state existed.

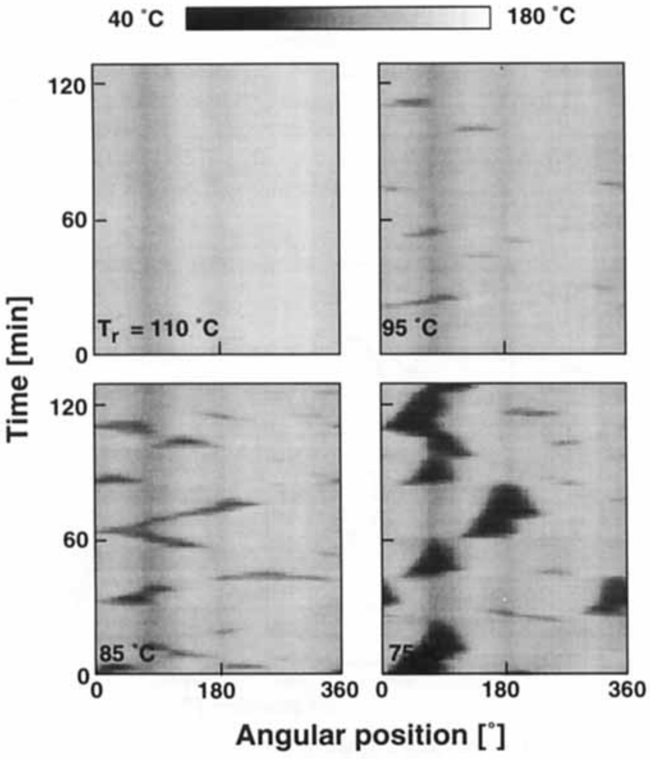

Figure 9. Expansion of the low temperature region upon reactor cooling for a feed containing 70 vol. % oxygen and 5 vol. % CO.

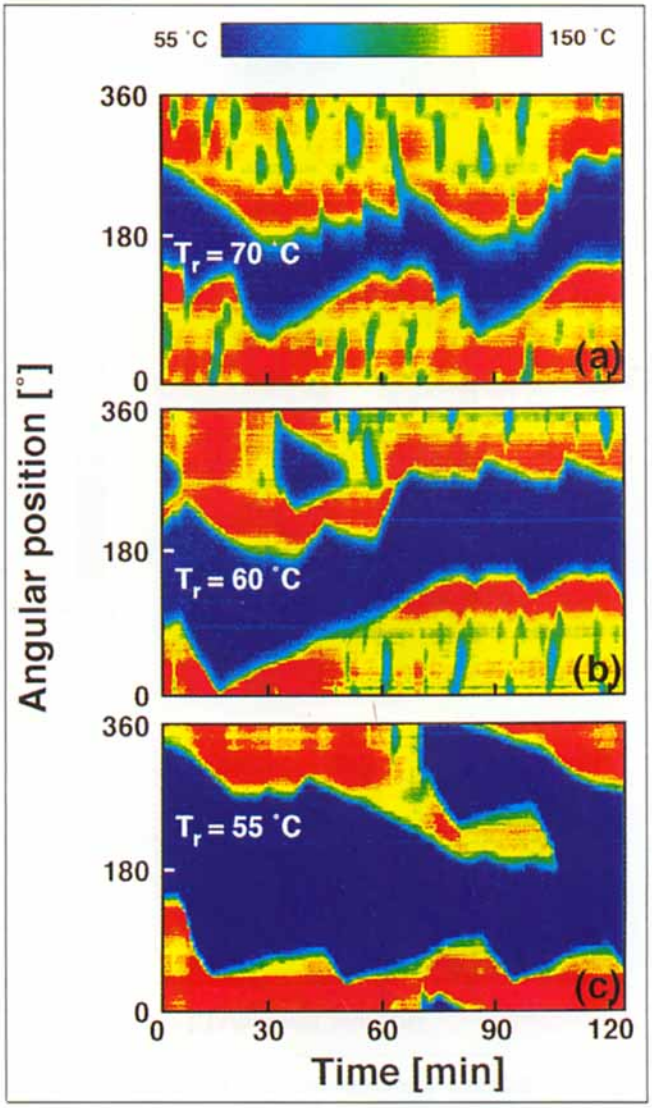

Figure 10. Surface temperature as a function of angular position and time for a feed containing 70 vol. % oxygen and 5 vol. % CO with a reactor temperature of (a) 70°C; (b) 60°C; (c) 55°C.

Discussion

The shape of the region of bistable uniform states in the reactor CO concentration vs. temperature map (Figure 13) was affected by the inhibitory effect of CO on the reaction rate and the heat release. This shape is similar to those observed by previous investigators such as Garske and Harold (1992) for the reaction on Pt. The CO rate inhibition (Engel and Ertl, 1978; Ertl, 1981) increased the ignition temperature with increasing CO concentration. On the other hand, the higher temperature rise of the ignited states decreased the extinction temperature with increasing CO concentration. Thus, increasing the feed CO concentration expanded the range of reactor temperatures for which two uniform states existed (Figure 12). The shift of the ignition and extinction boundaries to the left with higher feed oxygen concentration (Figure 12) was caused by an increase in the rate due to the higher partial pressure of oxygen in the reactor.

The nonuniform states consisted of regions with high and low temperatures separated by rather sharp fronts. The high

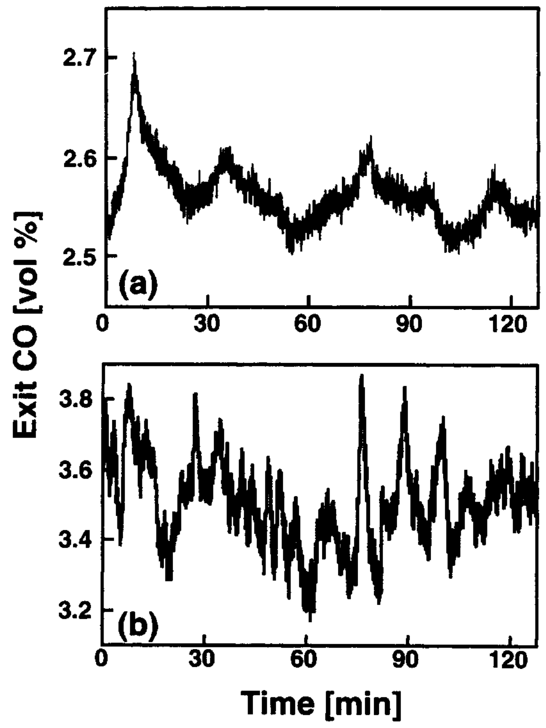

Figure 11. Dependence of reactor CO concentration on time for cases shown in (a) Figure 5a; (b) Figure 10a.

and low temperatures were very close to those of the uniformly ignited and extinguished states under the same reactor concentration. The nonuniform states were usually obtained for *feed* concentrations and reactor temperatures for which only uniformly extinguished states existed. However, both fully ignited and extinguished states existed for *reactor* concentrations and temperatures for which the nonuniform states were obtained (Figure 13). Note that different feed concentrations had to be used to get the same reactor concentration for a fully ignited, extinguished, or nonuniform state. For a given reactor concentration, the ignition and extinction temperatures of the nonuniform states were rather close to each other, in contrast to those for the uniform states. Moreover, the extinction temperature of the nonuniform state exceeded the ignition temperature.

The transition from the ignited branch to the nonuniform branch upon slow cooling for a feed containing 4 vol. % oxygen was associated with an extinction of part of the ring and a decrease in the overall reaction rate (Figures 2 and 3). The global interaction between the gas and the ring stabilized the nonuniform states under feed conditions for which a fully ignited state did not exist. For example, any attempt of the high-temperature region to reconquer the whole ring decreased the reactor CO concentration and the corresponding reaction rate. The decreased heat generation caused the front to slow down and retract. On the other hand, the global interaction prevented the expansion of the low-temperature region, as the gas concentration enabled part of the ring to remain ignited. The transition scenario from a fully ignited state to one with a low-temperature pulse (Figure 4) was similar to that observed during hydrogen oxidation on a ring-shaped supported nickel catalyst (Somani et al., 1996). This similarity indicates that the front's formation is generic for such exothermic, bistable catalytic systems in the presence of global coupling.

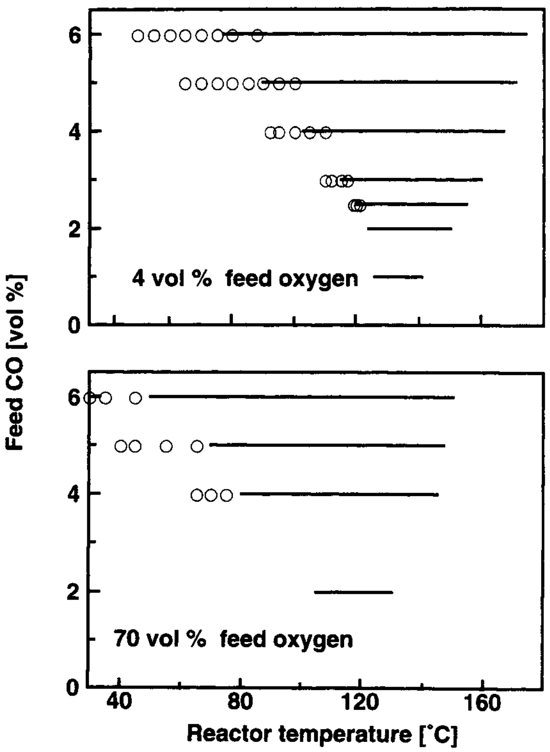

Figure 12. Map of regions with different qualitative behavior for a feed containing (a) 4 vol. % oxygen; (b) 70 vol. % oxygen.

The lines (open circles) denote uniform bistable states (a nonuniform state). The extreme right and left of the regions are the ignition and extinction boundaries, respectively.

Figure 14 shows heat generation and removal curves for two reactor temperatures. The heat removal is usually a linear function of the catalyst temperature. The heat generation is a nonlinear, sigmoidal function of the catalyst temperature. At high temperatures, it attains an asymptotic value proportional to the reactant concentration. For a single-variable system, a stable stationary front connecting high- and low-temperature states exists only if Eq. 1 is satisfied, that is, the two shaded areas in Figure 14 are equal. For a given reactor concentration, this condition is satisfied for one reactor temperature. Figure 13 shows that the range of reactor temperatures for which a nonuniform state exists at a given reactor concentration was very narrow, in close agreement with the preceding prediction.

A decrease in the feed concentration does not influence the heat-removal line. Thus, in order for condition (1) to be satisfied, the reactor concentration has to be the same for all feed concentrations This implies that the feed concentration affects the length of the region bounded by the two temperature fronts, but neither the temperatures of the hot and cold zones nor the effluent concentration. In our experiments, the change in the temperatures of the hot and cold regions was indeed small for different feed CO concentrations. However, the effluent concentration increased slightly with decreasing feed concentration (Figure 7). This may have been due to

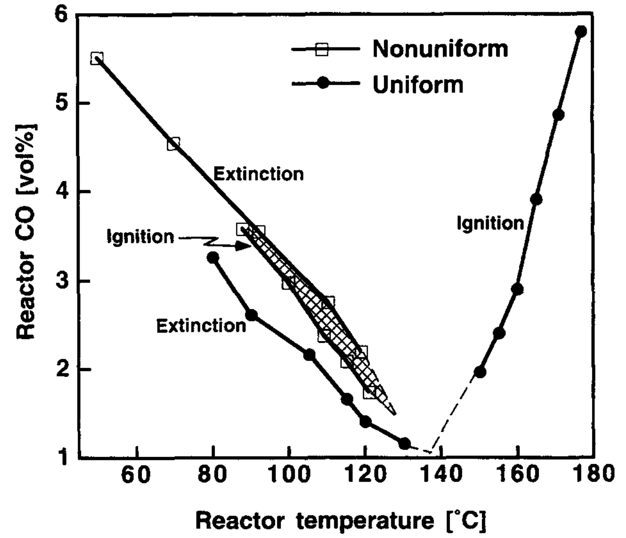

Figure 13. Regions with different qualitative behavior for a feed containing 4 vol. % oxygen in reactor concentration vs. reactor temperature map.

The lines with filled circles (open squares) denote ignition and extinction boundaries of uniform states (nonuniform state).

either ring nonuniformity, a slight decrease in the reactor temperature, or an increase in the oxygen concentration as the feed CO concentration was decreased. It should be noted that the single-variable model did not adequately describe the impact of the concentration change during hydrogen oxidation experiments (Somani et al., 1996).

Decreasing the reactor temperature shifts the heat-removal line to the left (Figure 14), so that Eq. 1 can be satisfied only at a higher reactor concentration, that is, the fraction of the ring occupied by the low reaction rate (low temperature) expands. This increases the temperature of the hot spot. This predicted response was observed in our experiments (Figure 6) as well as during hydrogen oxidation on a supported nickel catalyst (Somani et al., 1996). The equal-area condition does not provide a general answer whether the temperature of the high-temperature region will increase or decrease, as this depends on the relative positions of the points C and D.

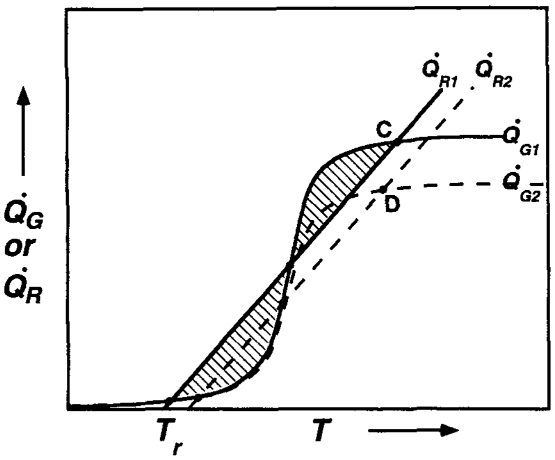

Figure 14. Heat generation and removal curves.

A temperature front connecting an ignited and extinguished region is stable only when the two hatched areas are equal (Eq. 1). To satisfy this condition the reactor concentration has to decrease as the reactor temperature is increased.

We define the length of the temperature front, w, as $\Delta T_{\max}/(dT/dx)_{\max}$, where $\Delta T_{\max}$ is the difference between the maximum and minimum temperature, and $(dT/dx)_{\max}$ is the temperature gradient at the inflection point. The front length is in general about three to four times the characteristic thermal length-scale of the catalyst (Barelko et al., 1978) which is,

$$L_h = \sqrt{\frac{k_s}{h}\frac{A}{P}}, \tag{2}$$

with k_s being the thermal conductivity of the solid [0.25 $\text{J}\cdot\text{m}^{-1}\cdot\text{s}^{-1}\cdot\text{K}^{-1}$ (Satterfield, 1991)], A the catalyst cross section ($3.6\times10^{-6}\text{m}^2$), and P the perimeter of cross section ($8.2\times10^{-3}\text{m}$). The heat-transfer coefficient, h, was determined experimentally to be 60 $\text{J}\cdot\text{m}^{-2}\cdot\text{s}^{-1}\cdot\text{K}^{-1}$. Equation 2 yields $L_h = 0.14$ cm, that is, a front length of 0.40–0.55 cm, in good agreement with our observations (0.4–0.6 cm). This front length was essentially independent of the operating conditions and was much smaller than that observed (1.3–1.5 cm) during hydrogen oxidation on a supported nickel ring (Somani et al., 1996). The high thermal transport through the gas phase in the hydrogen oxidation experiments was probably the main cause for the increase in the length of the front; the impact of the gas-phase heat transport was much lower in the CO oxidation reaction, as the thermal diffusivities of CO, oxygen, and nitrogen are 6–7 times smaller than that of hydrogen (Bird et al., 1960).

The temperature fronts continuously migrated back-and-forth on the ring in a nonperiodic manner, unlike the stationary fronts formed during hydrogen oxidation on a supported nickel catalyst (Somani et al., 1996). Back-and-forth-moving pulses had been observed previously during the oscillatory propylene oxidation on an electrically heated Pt ribbon, the average temperature of which was held constant (Philippou et al., 1991; Philippou and Luss, 1993). In extensive simulations on a uniformly active ring catalyst, Middya et al. (1994) did not observe back-and-forth-moving temperature fronts. However, Rinzel and Terman (1982) predicted that in bistable systems, fronts moving with different velocities and in opposite directions may exist. This was confirmed experimentally by Haas et al. (1995). When a spatial variation causes a qualitative change in the local dynamics, a front may move into a region where its motion is unstable and suddenly transform into a front traveling in the other direction (Hagberg et al., 1996; Liauw et al., 1996a).

We believe that the back-and-forth motion was induced by some nonuniformity of the catalyst. This conjecture is supported by the fact that the fronts reversed their motion at locations where the temperature profile of the fully ignited state was steep (Figure 5), similar to the behavior expected from the simulations by Hagberg et al. (1996) and Liauw et al. (1996a). The nonuniformity may have been introduced either by a nonuniform catalyst activity or nonuniform flow. We conjecture that flow maldistribution was the major cause of the nonuniformity, as the temperature profile of the ignited state was not affected by a 180° rotation of the ring.

One should distinguish between the nonuniformity of the surface temperature of the patterned states and of the fully ignited states. While the latter reflects the spatial variation of the system properties, the former is due to the bistability of the system, global coupling, and the spatial variation in the system properties. Theory predicts that either stationary or moving fronts may form in uniform systems. However, while pulses rotate on a uniform ring, they may exhibit other motions, such as a back-and-forth movement, on a nonuniform one (Liauw et al., 1996a; Hagberg et al., 1996).

The front motions were affected by the nonuniformity of the system and the global coupling. It is very difficult to separate the impact of these two influences on the observed motions. The global coupling caused the movement of each front to affect that of the other front(s) and encouraged both fronts to move in the same direction and at similar velocities, as observed in Figure 5a (feed with 4 vol. % oxygen). However, for a feed of 70 vol. % oxygen, the ignition and extinction fronts moved with different velocities and sometimes even in the opposite directions (Figure 10). This motion was due to the nonuniformity of the system.

The impact of the nonuniformity depends on the local dynamic features and the activity profiles. For a system with synclinal bistability, the nonuniformity tends to arrest front motion and leads to stationary fronts (Liauw et al., 1996a). Global coupling may also arrest front motion in uniform bistable systems (Middya et al., 1994). Such a stationary high-temperature region was observed by Somani et al. (1996) during hydrogen oxidation on a supported Ni catalyst. An anticlinal bistability leads to multiplicity of front velocity. In a ring-shaped system, one may find rotating pulses or, in the presence of nonuniformities, back-and-forth movement of pulses. We conjecture that anticlinal bistability plus nonuniformity was the cause of the patterns observed with 4 vol. % oxygen.

The local kinetics of the system containing 70 vol. % oxygen were more intricate. In addition to bistability at high reactor temperatures, the fully ignited state oscillated at lower reactor temperatures. Moreover, the smooth transition from the ignited to the nonuniform state was rather different from the discontinuous one for 4 vol. % oxygen. A remarkable feature of this system is the coexistence of fast-moving, low-amplitude moving cold spots (amplitude of 5–10 K, velocity of about 9 mm/min) and slow-moving, large-amplitude (50–100 K, velocity of 0.5–2.0 mm/min) temperature fronts (Figure 10). This behavior must be due to the impact of oxygen on the local kinetics. These moving cold spots were superimposed on the high-temperature regions and led to fast oscillations of the reaction rate (Figure 11b). This behavior is reminiscent of the local cooling described by Qin and Wolf (1995), Liauw et al. (1996b), and Yamamoto et al. (1995a). Under some conditions, the cooling occurred almost simultaneously over the entire ring, while the reheating appeared to propagate in a wavelike motion. This agrees with the observations by Qin and Wolf (1995).

The small-amplitude (5–10 K) of the local temperature oscillations suggest a kinetic mechanism rather than a thermokinetic one. A cyclic formation and depletion of a subsurface oxygen layer, suggested by Ladas et al. (1989), has been used in models (Bassett and Imbihl, 1990; Hartmann et al., 1994) for the reaction at low pressures. *In-situ* X-ray absorption on Pd supported catalyst suggested that a cyclic oxidation and reduction mechanism occurs even at atmospheric pressure (Ressler, 1995). The onset of oscillations upon the increase of oxygen concentration may indicate a similar mechanism in our system. However, the pronounced nonisothermicity does not allow for a straightforward application of the subsurface oxygen model.

The patterns were usually observed for feed concentrations, for which the only uniform state that existed at the reactor temperature was an extinguished state. The conversion attained by the nonuniform state always exceeded that of the extinguished one. However, it did not exceed that of a fully ignited state. It is still an open question whether and for which reaction and operating conditions a patterned state will give a higher yield of the desired product than any uniform state at the same reactor conditions. We speculate that this may happen in equilibrium-limited reactions for which the time constant of the rate-limiting step is of the order of the moving temperature fronts.

Acknowledgments

This work was supported by grants from the National Science Foundation, the Welch Foundation, the Deutsche Forschungsgemeinschaft, and NATO.

Literature Cited

Bangia, A. K., M. Bär, I. G. Kevrekidis, M. D. Graham, H.-H. Rotermund, and G. Ertl, "Catalysis on Microcomposite Surfaces," *Chem. Eng. Sci.*, **51**, 1757 (1996).

Bär, M., M. Hildebrand, M. Eiswirth, M. Falcke, H. Engel, and M. Neufeld, "Chemical Turbulence and Standing Waves in a Surface Reaction Model: The Influence of Global Coupling and Wave Instabilities," *CHAOS*, **4**, 499 (1994).

Barelko, V., I. I. Kurochka, A. G. Merzhanov, and K. G. Shkadinskii, "Investigation of Traveling Waves on Catalytic Wires," *Chem. Eng. Sci.*, **33**, 805 (1978).

Bassett, M. R., and R. Imbihl, "Mathematical Modelling of Kinetic Oscillations in the Catalytic CO Oxidation on Pd (110): The Subsurface Oxygen Model," *J. Chem. Phys.*, **93**, 811 (1990).

Beusch, H., P. Fieguth, and E. Wicke, "Thermisch und kinetisch verursachte Instabilitäten im Reaktionsverhalten einzelner Katalysatorkörner," *Chem. Ing. Tech.*, **44**, 445 (1972).

Bird, R. B., W. E. Stewart, and E. N. Lightfoot, *Transport Phenomena*, Wiley, New York (1960).

Brown, J. R., G. A. D'Netto, and R. A. Schmitz, "Spatial Effects and Oscillations in Heterogeneous Catalytic Reactions," *Temporal Order*, L. Rensing and N. I. Jaeger, eds., Springer-Verlag, Berlin p. 86 (1985).

Busch, H., "Über die Erwärmung von Drähten in verdünnten Gasen durch den elektrischen Strom," *Ann. Phys.*, **64**, 401 (1921).

Castets, V., E. Dulos, J. Boissonade, and P. De Kepper, "Experimental Evidence of a Sustained Standing Turing-Type Nonequilibrium Chemical Pattern," *Phys. Rev. Lett.*, **64**, 2953 (1990).

Choi, K. I., and M. A. Vannice, "CO Oxidation over Pd and Cu Catalysts: III. Reduced Al_2O_3-Supported Pd," *J. Catal.*, **131**, 1 (1991).

Cordonier, G. A., and L. D. Schmidt, "Thermal Waves in NH_3 Oxidation on a Pt Wire," *Chem. Eng. Sci.*, **44**, 1983 (1989).

Cordonier, G. A., F. Schüth, and L. D. Schmidt, "Oscillations in Methylamine Decomposition on Pt, Rh, and Ir: Experiments and Model," *J. Chem. Phys.*, **91**, 5374 (1989).

Cross, M. C., and P. C. Hohenberg, "Pattern Formation Outside of Equilibrium," *Rev. Mod. Phys.*, **65**, 851 (1993).

Engel, T., and G. Ertl, "A Molecular Beam Investigation of the Catalytic Oxidation of CO on Pd (111)," *J. Chem. Phys.*, **69**, 1267 (1978).

Ertl, G., "Kinetics of Chemical Processes on Well-Defined Surfaces," *Catalysis: Science and Technology*, J. R. Anderson and M. Boudart, eds., Springer-Verlag, Berlin (1981).

Ertl, G., "Oscillatory Catalytic Reactions at Single-Crystal Surfaces," *Adv. Catal.*, **37**, 213 (1990).

Ertl, G., "Oscillatory Kinetics and Spatio-Temporal Self-Organization in Reactions at Solid Surfaces," *Science*, **254**, 1750 (1991).

Ertl, G., and R. Imbihl, "Oscillatory Kinetics in Heterogeneous Catalysis," *Chem. Rev.*, **95**, 697 (1995).

Garske, M. E., and M. P. Harold, "Observed Kinetics of an Exothermic Reaction on a Temperature-Controlled Catalytic Wire," *Chem. Eng. Sci.*, **47**, 623 (1992).

Graham, M. D., S. L. Lane, and D. Luss, "Temperature Pulse Dynamics on a Catalytic Ring," *J. Phys. Chem.*, **97**, 7564 (1993).

Graham, M. D., I. G. Kevrekidis, K. Asakura, J. Lauterbach, K. Krischer, H.-H. Rotermund, and G. Ertl, "Effects of Boundaries on Pattern Formation: Catalytic Oxidation of CO on Platinum," *Science*, **264**, 80 (1994).

Haas, G., M. Bär, I. G. Kevrekidis, P. B. Rasmussen, H.-H. Rotermund, and G. Ertl, "Observation of Front Bifurcations in Controlled Geometries: From One to Two Dimensions," *Phys. Rev. Lett.*, **75**, 3560 (1995).

Hagberg, A., E. Meron, I. Rubinstein, and B. Zaltzman, "Controlling Domain Patterns Far from Equilibrium," *Phys. Rev. Lett.*, **76**, 427 (1996).

Hartmann, N., K. Krischer, R. Imbihl, "The Role of Adsorbate-Adsorbate Interactions in the Rate Oscillations in Catalytic CO Oxidation on Pd (110)," *J. Chem. Phys.*, **101**, 6717 (1994).

Jaeger, N. I., K. Möller, and P. J. Plath, "Cooperative Effects in Heterogeneous Catalysis: I. Phenomenology of the Dynamics of Carbon Monoxide Oxidation on Palladium Embedded in a Zeolite Matrix," *J. Chem. Soc., Faraday Trans. 1*, **82**, 3315 (1986).

Kaul, D. J., and E. E. Wolf, "Selected Area Fourier Transform Infrared Studies of Surface Reaction Dynamics: III. Spatial Coverage and Temperature Patterns during Self-sustained Oscillations of CO Oxidation on Pd/SiO_2," *J. Catal.*, **93**, 321 (1985).

Kellow, J. C., and E. E. Wolf, "Infrared Thermography and FTIR Studies of Catalyst-preparation Effects on Surface-Reaction Dynamics during CO and Ethylene Oxidation on Rh/SiO_2 Catalysts," *Chem. Eng. Sci.*, **45**, 2597 (1990).

Kellow, J. C., and E. E. Wolf, "Propagation of Oscillations during Ethylene Oxidation on a Rh/SiO_2 Catalyst," *AIChE J.*, **37**, 1844 (1991).

Kulka, A., M. Bode, and H.-G. Purwins, "On the Influence of Inhomogeneities in a Reaction-Diffusion System," *Phys. Lett. A*, **203**, 33 (1995).

Ladas, S., R. Imbihl, and G. Ertl, "Kinetic Oscillations during the Catalytic CO Oxidation on Pd (110): The Role of Subsurface Oxygen," *Surf. Sci.*, **219**, 88 (1989).

Lane, S. L., and D. Luss, "Rotating Temperature-pulse during Hydrogen Oxidation on a Nickel Ring," *Phys. Rev. Lett.*, **70**, 830 (1993).

Lane, S. L., M. D. Graham, and D. Luss, "Spatiotemporal Temperature Patterns during Hydrogen Oxidation on a Nickel Disk," *AIChE J.*, **39**, 1497 (1993).

Lee, K.-J., W. D. McCormick, Q. Ouyang, and H. L. Swinney, "Pattern Formation by Interacting Chemical Fronts," *Science*, **261**, 192 (1993).

Liauw, M. A., J. Ning, and D. Luss, "Pattern Formation on a Nonuniformly Active Ring," *J. Chem. Phys.*, **104**, 5657 (1996a).

Liauw, M. A., P. J. Plath, and N. I. Jaeger, "Complex Oscillations and Global Coupling during the Catalytic Oxidation of CO," *J. Chem. Phys.*, **104**, 6375 (1996b).

Lobban, L., and D. Luss, "Spatial Temperature Oscillations during Hydrogen Oxidation on a Nickel Foil," *J. Phys. Chem.*, **93**, 6530 (1989).

Lobban, L., G. Philippou, and D. Luss, "Standing Temperature Waves on Electrically Heated Catalytic Ribbons," *J. Phys. Chem.*, **93**, 733 (1989).

Lynch, D. T., and S. E. Wanke, "Oscillations during CO Oxidation over Supported Metal Catalysts: I. Influence of Catalyst History on Activity," *J. Catal.*, **88**, 333 (1984).

Middya, U., M. Sheintuch, M. D. Graham, and D. Luss, "Patterns of Temperature Pulses on Electrically Heated Catalytic Ribbons," *Physica D*, **63**, 393 (1993).

Middya, U., D. Luss, and M. Sheintuch, "Spatiotemporal Motions Due to Global Interaction," *J. Chem. Phys.*, **100**, 3568 (1994).

Middya, U., and D. Luss, "Impact of Global Interaction on Pattern Formation on a Disk," *J. Chem. Phys.*, **102**, 5029 (1995).

Mikhailov, A. S., *Foundations of Synergetics I: Distributed Active Systems*, Springer-Verlag, Berlin (1990).

Pawlicki, P. C., and R. A. Schmitz, "Spatial Effects on Supported Catalysts," *Chem. Eng. Prog.*, **83**, 40 (1987).

Philippou, G., F. Schultz, and D. Luss, "Spatiotemporal Temperature Patterns on an Electrically Heated Catalytic Ribbon," *J. Phys. Chem.*, **95**, 3224 (1991).

Philippou, G., and D. Luss, "Temperature Patterns on a Catalytic Ribbon Heated by a Constant Voltage," *Chem. Eng. Sci.*, **48**, 2313 (1993).

Pismen, L. M., "Asymmetric Steady States Revisited," *Chem. Eng. Sci.*, **34**, 563 (1979).

Plichta, R. T., and R. A. Schmitz, "Oscillations in the Oxidation of Carbon Monoxide on a Platinum Foil," *Chem. Eng. Commun.*, **3**, 387 (1979).

Qin, F., and E. E. Wolf, "Infrared Thermography Studies of Unsteady-State Processes during CO Oxidation on Supported Catalysts," *Chem. Eng. Sci.*, **49**, 4263 (1994).

Qin, F., and E. E. Wolf, "Vibrational Control of Chaotic Self-Sustained Oscillations during CO Oxidation on a Rh-SiO_2 Catalyst," *Chem. Eng. Sci.*, **50**, 117 (1995).

Ressler, T., "Application of Energy-Dispersive X-Ray Absorption Spectroscopy in Heterogeneous Catalysis: Exfoliation of Graphite Intercalation Compounds and Oscillatory Behavior in the CO Oxidation," PhD Thesis, Univ. Hamburg, Hamburg, Germany (1995).

Rinzel, J., and D. Terman, "Propagation Phenomena in a Bistable Reaction-Diffusion System," *SIAM J. Appl. Math.*, **42**, 1111 (1982).

Satterfield, C. N., *Heterogeneous Catalysis in Industrial Practice*, McGraw-Hill, New York (1991).

Schüth, F., B. E. Henry, and L. D. Schmidt, "Oscillatory Reactions in Heterogeneous Catalysis," *Adv. Catal.*, **39**, 51 (1993).

Schütz, P., M. Bode, and H.-G. Purwins, "Bifurcations of Front Dynamics in a Reaction-Diffusion System with Spatial Inhomogeneities," *Physica D*, **82**, 382 (1995).

Sheintuch, M., "Spatio-temporal Structures of Controlled Catalytic Wires," *Chem. Eng. Sci.*, **44**, 1081 (1989).

Sheintuch, M., and J. Schmidt, "Bifurcations to Periodic and Aperiodic Solutions during Ammonia Oxidation on a Pt Wire," *J. Phys. Chem.*, **92**, 3404 (1988).

Sheintuch, M., and S. Shvartsman, "Spatiotemporal Patterns in Catalytic Reactors," *AIChE J.*, **42**, 1041 (1996).

Slin'ko, M. M., and N. I. Jaeger, *Oscillating Heterogeneous Catalytic Systems*, Elsevier, Amsterdam (1994).

Slin'ko, M. M., N. I. Jaeger, and P. Svensson, "Mechanism of the Kinetic Oscillations in the Oxidation of CO on Palladium Dispersed within a Zeolite Matrix," *J. Catal.*, **118**, 349 (1989).

Somani, M., M. A. Liauw, and D. Luss, "Hot Spot Formation on a Catalyst," *Chem. Eng. Sci.*, **51**, 4259 (1996).

Somani, M., "Nonuniform Temperature Patterns in Various Catalytic Systems," PhD Diss., Univer. of Houston, Houston, TX (1996).

Somani, M., M. A. Liauw, and D. Luss, "Evolution and Impact of Temperature Patterns during Hydrogen Oxidation on a Ni Ring," *Chem. Eng. Sci.*, in press (1997).

Volodin, Y. E., Barelko, V. V., and P. I. Khalzov, "Investigation of Instability of Oxidation of H_2 and $NH_3 + H_2$ on Platinum," *Chem. Eng. Commun.*, **18**, 271 (1982).

Yamamoto, S. Y., C. M. Surko, M. B. Maple, and R. K. Pina, "Pulse Propagation in the Catalytic Oxidation of Carbon Monoxide on Platinum," *Phys. Rev. Lett.*, **74**, 4071 (1995a).

Yamamoto, S. Y., C. M. Surko, M. B. Maple, and R. K. Pina, "Spatio-Temporal Dynamics of Oscillatory Heterogeneous Catalysis: CO Oxidation on Platinum," *J. Chem. Phys.*, **102**, 8614 (1995b).

Zaikin, A. N., and A. M. Zhabotinskii, "Concentration Wave Propagation in Two-Dimensional Liquid-Phase Self-Oscillating System," *Nature*, **225**, 535 (1970).

Manuscript received Oct. 7, 1996, and revision received Feb. 19, 1997.